Clinical Science (2023) **137** 697–706
https://doi.org/10.1042/CS20220753

PORTLAND PRESS

Research Article

Increased methylglyoxal formation in plasma and tissues during a glucose tolerance test is derived from exogenous glucose

Xiaodi Zhang[1,2], Jean L.J.M. Scheijen[1,2], Coen D.A. Stehouwer[1,2], Kristiaan Wouters[1,2] and Casper G. Schalkwijk[1,2]

[1]Department of Internal Medicine, Maastricht University Medical Center, Maastricht 6229ER, the Netherlands; [2]Department of Internal Medicine, CARIM School for Cardiovascular Diseases, Maastricht University, Maastricht 6229ER, the Netherlands

Correspondence: Casper G. Schalkwijk (C.Schalkwijk@maastrichtuniversity.nl)

The dicarbonyl compound methylglyoxal (MGO) is a major precursor in the formation of advanced glycation endproducts (AGEs). MGO and AGEs are increased in subjects with diabetes and are associated with fatal and nonfatal cardiovascular disease. Previously, we have shown that plasma MGO concentrations rapidly increase in the postprandial phase, with a higher increase in individuals with type 2 diabetes. In current study, we investigated whether postprandial MGO formation in plasma and tissues originates from exogenous glucose and whether the increased plasma MGO concentration leads to a fast formation of MGO-derived AGEs.

We performed a stable isotope-labelled oral glucose tolerance test (OGTT) in 12 healthy males with universally labelled D(+)^{13}C glucose. Analysis of plasma-labelled $^{13}C_3$ MGO and glucose levels at 11 time-points during the OGTT revealed that the newly formed MGO during OGTT is completely derived from exogenous glucose. Moreover, a fast formation of protein-bound MGO-derived AGEs during the OGTT was observed. In accordance, *ex-vivo* incubation of MGO with plasma or albumin showed a rapid decrease in MGO and a fast increase in MGO-derived AGEs. In an intraperitoneal glucose tolerance test in C57BL/6J mice, we confirmed that the formation of postprandial MGO is derived from exogenous glucose in plasma and also showed in tissues that MGO is increased and this is also from exogenous glucose.

Collectively, increased formation of MGO during a glucose tolerance test arises from exogenous glucose both in plasma and in tissues, and this leads to a fast formation of MGO-derived AGEs.

Introduction

Methylglyoxal (MGO) is a highly reactive dicarbonyl compound and spontaneously modifies amino groups in protein. MGO is a major precursor in the formation of advanced glycation endproducts (AGEs) [1] such as Nδ-(5-hydro-5-methyl-4-imidazolon-2-yl)-ornithine (MG-H1) and N$^{\varepsilon}$-(carboxyethyl)lysine (CEL) [2–4]. MGO and MGO-derived AGEs have detrimental effects on cellular function [5–7], inflammation, and cell death [8–10], are increased in subjects with type 1 and 2 diabetes and are associated with fatal and nonfatal cardiovascular disease [8,11–15]. We have recently shown that plasma MGO concentrations rapidly increased both during an oral glucose tolerance test (OGTT) and a mixed meal test, with a higher increase in individuals with type 2 diabetes [16,17]. Since MGO is rapidly formed postprandially, repeated episodes of elevated MGO plasma concentration may lead to MGO stress, and may contribute to the detrimental effects of postprandial glucose spikes [18].

Received: 08 November 2022
Revised: 22 December 2022
Accepted: 19 January 2023

Accepted Manuscript online: 20 January 2023
Version of Record published: 26 April 2023

Clinical Science (2023) **137** 697–706
https://doi.org/10.1042/CS20220753

MGO is mainly formed from glycolysis-derived triose phosphates [19,20], but minor sources are degradation of glycated proteins, oxidation of acetone, and lipid peroxidation [13]. The exact source of the postprandial MGO in plasma is unknown. Therefore, we investigated *in-vivo* whether postprandial MGO directly originates from exogenous glucose during an OGTT in healthy humans, using universally labelled D(+)^{13}C glucose, and in mice whether MGO increased in tissues after a GTT. Furthermore, we investigated *in-vitro* whether the MGO leads to a rapid formation of plasma MGO-derived AGEs.

Materials and methods

Human study

A total of 12 healthy males, with an average age of 25 years (range 21–30 years) and average BMI of 22.5 kg/m^2 (range: 19.2–24.7 kg/m^2) were recruited. No medication use was reported by the subjects. Approval was obtained from the Medical Ethics Committee Brabant (Tilburg, The Netherlands) on 1 December 2015. Each subject provided written informed consent for the study. This trial was registered at controlled-trials.com as ISRCTN42106325.

Experimental design

After an overnight fasting period, study participants underwent a stable isotope-labelled OGTT with 50 g glucose of which 2% was universally labelled D(+)^{13}C glucose, enabling us to track the occurrence of labelled $^{13}C_3$ MGO, which we refer to as formation of MGO, in the obtained samples. Blood samples were collected at 11 time-points after the intake of glucose: every 15 min for first 2 h and every half an hour for the next 4 h. Concentrations of MGO and glucose in plasma during OGTT (6 h) were measured at 11 time-points with ultra-performance liquid chromatography-tandem mass spectrometry (UPLC-MS/MS).

Measurements of MGO, free and protein-bound MGO-derived AGEs, and plasma glucose

MGO and MGO-derived AGEs in plasma were measured with UPLC-MS/MS (Waters, Milford, U.S.A.), as described in detail previously [21,22]. Plasma glucose concentrations were measured on a Roche/Hitachi Modular automatic analyser (Roche Diagnostics, Hitachi) by using a glucose hexokinase method. $^{13}C_3$ MGO and $^{13}C_6$ glucose data were corrected for a difference in mass spectrometry response factor between $^{13}C_3$ MGO and $^{12}C_3$ MGO, and between $^{13}C_6$ glucose and $^{12}C_6$ glucose, respectively.

It was assumed that labelled and unlabelled glucose molecules showed identical behaviour. Based on the 2% dose of the total of 50 g glucose, the appearance of total $^{13}C_6$ glucose and $^{13}C_3$ MGO was corrected for dose.

Ex-vivo experiments

Bovine serum albumin (BSA, 50 g/l in PBS) and human plasma from healthy donors was incubated at 37°C for 0, 1, 2, 3, 4, 5, 6, 8, and 24 h with 0, 1, 10, and 100 μmol/l MGO. MGO was produced as previously described [23]. Every sample was snap frozen in liquid nitrogen and stored at −80°C until analysis. Protein-bound MG-H1 and CEL levels and MGO concentrations were measured with UPLC-MS/MS (Waters, Milford, U.S.A.) [21,22].

Mouse experiments

Four-week-old male C57BL/6J mice were purchased from Charles River Europe and were maintained in the animal facility until the age of 10–12 weeks, with four mice per cage. Mice were fasted overnight for 16 h and received an intraperitoneal glucose tolerance test (IPGTT) with a solution of universally labelled D(+) ^{13}C glucose (Sigma-Aldrich), 2 g/kg body weight dissolved in saline. These mice were euthanised by means of CO_2/O_2 mixture at either 30, 60, or 120 min after the glucose injection, respectively. The control group of mice received no treatment and were euthanised directly, at time 0 min of the IPGTT. Blood samples were collected from the heart in EDTA tubes and stored immediately on ice. Plasma samples were obtained after spinning the blood at 2000 ***g***, 4°C for 5 min, and were snap frozen and stored at −80°C until analysis. Pancreas, spleen, liver, kidney, visceral adipose tissue (VAT), subcutaneous adipose tissue (SAT), and skeletal muscle were collected, snap frozen and stored at −80°C. Glucose levels were measured in whole blood using a glucometer (Contour, Bayer, Leverkusen, Germany).

The experimental work protocol was approved by the local Animal Experiments Committee of Maastricht University, project license number AVD1070020187086. Experiments were performed at the Animal Laboratory of Internal Medicine, Maastricht University, by licensed people according to institutional guidelines.

Table 1 C_{max} and T_{max} of glucose and MGO

Parameter	C_{max}* (mean ± SEM, unit)	T_{max} (mean ± SEM, unit)
$^{12}C_6$ glucose	328114 ± 40611 (peak area MS)	41 ± 4.1 (min)
$^{13}C_6$ glucose	298345 ± 17997 (peak area MS)	50 ± 4.3 (min)
$^{12}C_3$ MGO	110.8 ± 11.8 (nmol/l)	48 ± 4.9 (min)
$^{13}C_3$ MGO	109.7 ± 6.5 (nmol/l)	56 ± 4.9 (min)

*$^{12}C_6$ glucose and $^{12}C_3$ MGO were corrected for baseline, $^{13}C_6$ glucose and $^{13}C_3$ MGO were corrected for dose (*50). Abbreviation: MS, mass spectrometry.

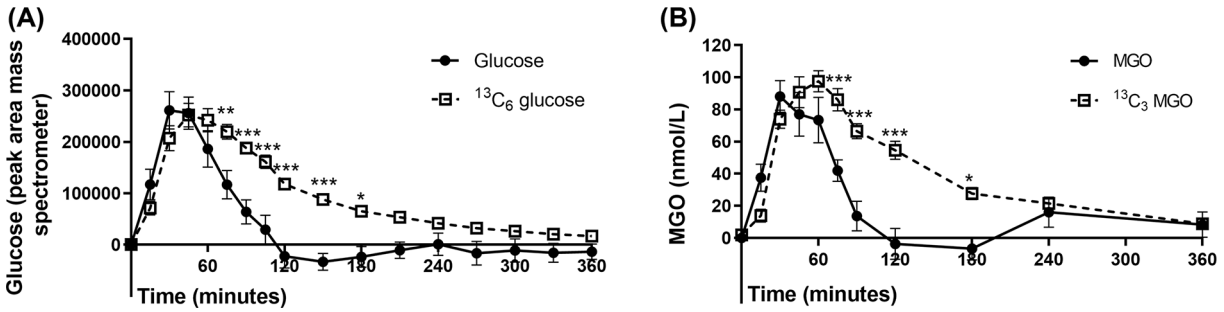

Figure 1. Plasma glucose and MGO concentrations during a stable isotope-labelled OGTT with universally labelled D(+)^{13}C glucose in humans

(**A**) Plasma glucose levels, and (**B**) plasma MGO concentrations were analysed by UPLC-MS/MS. $^{13}C_6$ glucose and $^{13}C_3$ MGO data were corrected for dose (*50) and for a difference in mass spectrometry response factor between $^{13}C_6$ glucose and $^{12}C_6$ glucose, $^{13}C_3$ MGO and $^{12}C_3$ MGO, respectively. $^{12}C_6$ Glucose and $^{12}C_3$ MGO levels were corrected for baseline. Data are shown as mean ± SEM, n=12. Comparisons of $^{13}C_6$ glucose and $^{12}C_6$ glucose, $^{13}C_3$ MGO and $^{12}C_3$ MGO over time were tested using two-way ANOVA with Tukey's multiple comparison. * represents comparisons with glucose or MGO at the same time point. * indicates $P<0.05$, ** indicates $P<0.01$, *** indicates $P<0.001$. Abbreviation: MGO, methylglyoxal.

Tissue preparations for measurements

Pancreas, spleen, liver, kidney, and skeletal muscle were homogenised by crushing in liquid nitrogen and dissolved in lysate buffer (0.1 M sodium phosphate buffer supplemented with 0.02% Triton-x (Sigma-Aldrich) and protease inhibitor (Roche)). VAT and SAT were homogenised with a Mini-bead beater homogeniser (Biospec), in the same lysate buffer as used for the other tissues. Concentrations of $^{13}C_3$ MGO and $^{12}C_3$ MGO were measured in homogenates of all tissue and plasma samples using UPLC-MS/MS, as described previously [21].

Statistical analysis

All data are presented as mean ± SEM. Statistical analysis were performed using GraphPad Prism 8.0.2. Two-way ANOVA with Bonferroni's multiple comparisons test was used to compare groups over time. One-way ANOVA with Tukey's multiple comparisons test was used to compare MGO and glucose levels between different time points. All analysis were considered statistically significant with P-values <0.05.

Results

Postprandial MGO formation in plasma during an OGTT is derived from exogenous glucose in humans

To investigate whether postprandial MGO formation directly originates from exogenous glucose, we performed an OGTT with 50 g glucose of which 2% was universally labelled D(+)^{13}C glucose. Plasma $^{12}C_6$ glucose levels increased rapidly after the glucose load with a calculated peak at 41 min, after which levels started to decline. The plasma $^{13}C_6$ glucose concentration showed a similar peak value as for $^{12}C_6$ glucose. However, the decline of $^{13}C_6$ glucose levels after the peak was significantly slower than for $^{12}C_6$ glucose (Table 1 and Figure 1A). After 180 min postload, plasma $^{12}C_6$ glucose, but not $^{13}C_6$ glucose, slightly increased (Figure 1A). The curves of plasma $^{12}C_3$ MGO and $^{13}C_3$ MGO followed the same pattern as observed for $^{12}C_6$ glucose and $^{13}C_6$ glucose, respectively. Plasma $^{12}C_3$ MGO and $^{13}C_3$

Clinical Science (2023) **137** 697–706
https://doi.org/10.1042/CS20220753

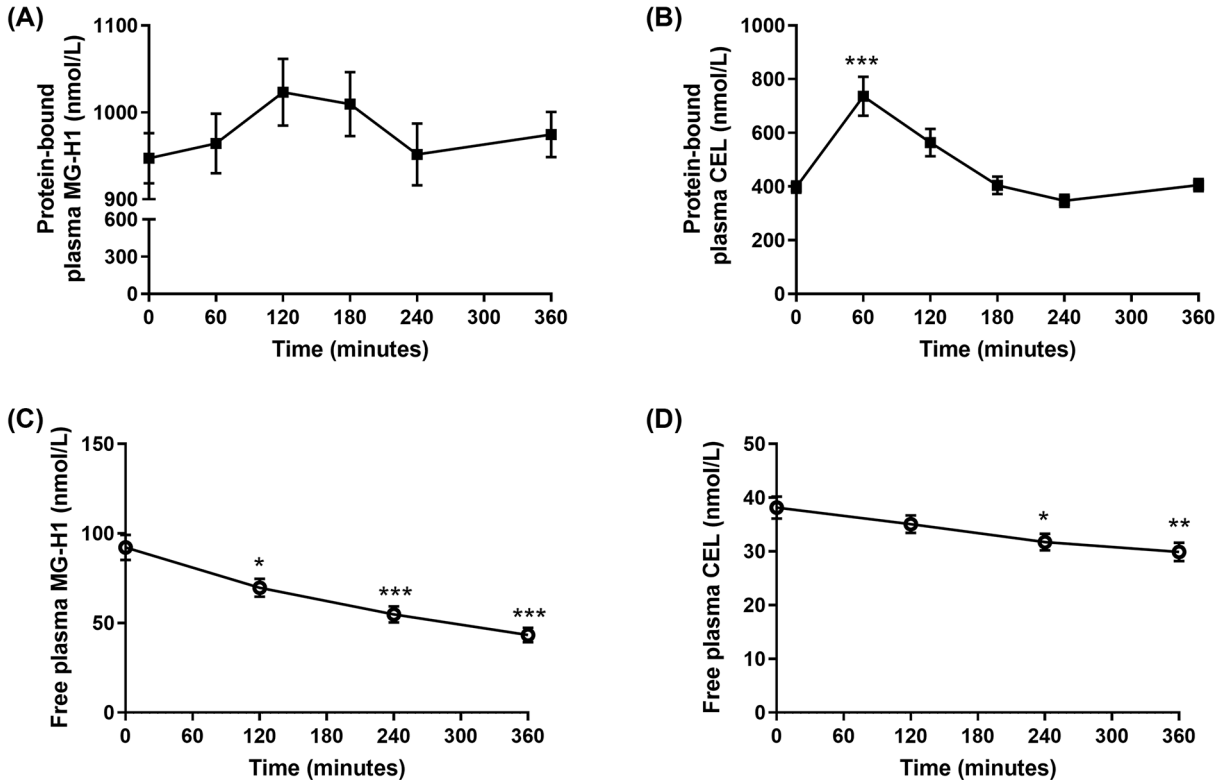

Figure 2. MGO-derived AGEs concentrations in plasma during an OGTT in humans

(**A**) Protein-bound plasma MG-H1, (**B**) protein-bound plasma CEL, (**C**) free plasma MG-H1, and (**D**) free plasma CEL were analysed by UPLC-MS/MS. Data are shown as mean ± SEM, n=12. Comparisons of protein-bound and free AGEs levels at different time points were tested using one-way ANOVA with Tukey's multiple comparison. * represents comparisons with time 0. * indicates $P<0.05$, ** indicates $P<0.01$, *** indicates $P<0.001$. Abbreviations: CEL, N^{ε}-(carboxyethyl)lysine; MG-H1, Nδ-(5-hydro-5-methyl-4-imidazolon-2-yl)-ornithine.

MGO showed a rapid increase with a calculated C_{max} at 49 and 56 min, respectively (Table 1 and Figure 1B). After 180 min, $^{12}C_3$ MGO slightly increased (Figure 1B). Collectively, these data show that the rapid increase in MGO formation is completely derived from exogenous glucose during the 6-h OGTT.

Postprandial protein-bound AGEs formation in plasma increases rapidly during an OGTT in humans

Since MGO can react rapidly with proteins to form AGEs [24], we next investigated the formation of postprandial MGO-derived AGEs in plasma during the 6h OGTT. Plasma protein-bound CEL increased after a glucose load and reached a peak 60 min (+85%; $P<0.001$). Plasma protein-bound MG-H1 showed the highest levels after 120 min (+8%; $P=0.36$), but this was not statistically significant. For both MGO-derived AGEs, the concentrations decreased and the lowest concentrations were found at 240 min during the OGTT, after which the concentrations slightly increased again (Figure 2A,B). In contrast with protein-bound AGEs, the concentrations of free plasma MG-H1 and CEL continuously decreased during the entire 6h OGTT (Figure 2C,D).

MGO rapidly induces AGEs formation in plasma *ex vivo*

We next investigated whether these MGO-derived AGEs can be directly formed by MGO in plasma. The incubation of human plasma with different concentrations of MGO *ex vivo* for 24 h, induced a time- and dose-dependent increase in protein-bound MG-H1 and CEL, which occurred rapidly during the first 6 h (Figure 3A,B). After 6 h, the levels of protein-bound MG-H1 and CEL continued to increase, albeit at a slower rate.

The incubation of BSA with MGO resulted in a similar pattern for protein-bound MG-H1 formation as in plasma, while protein-bound CEL formation was not induced by MGO (Figure 3C,D). The incubation of BSA with 10 and 100 μM MGO showed a fast decrease in MGO levels during the first 6 h (Figure 3E,F), demonstrating the high reactivity of MGO with proteins.

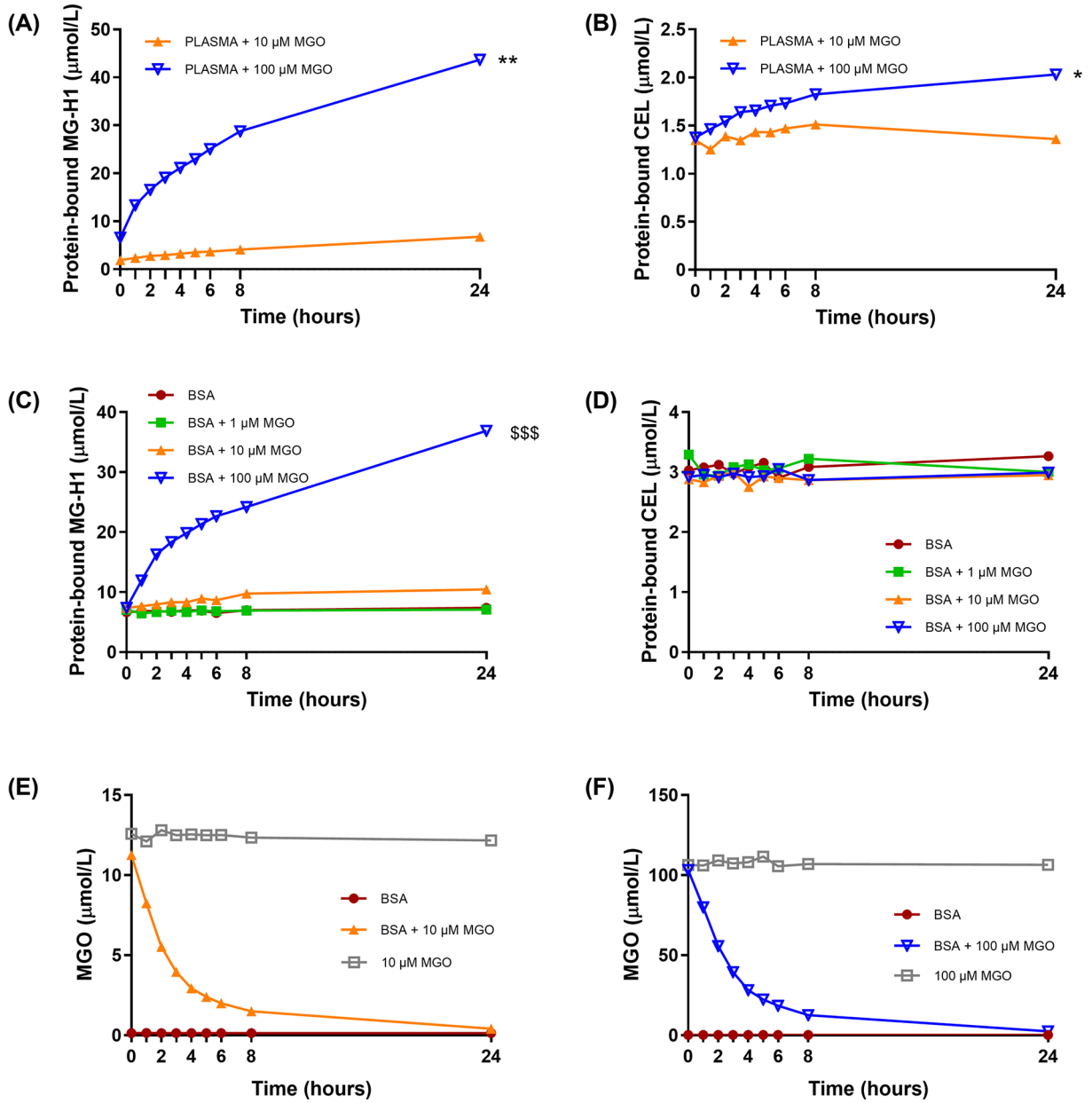

Figure 3. Protein-bound AGE formation in plasma and BSA after incubating with MGO *ex vivo*

The concentrations of (**A**) protein-bound plasma MG-H1, (**B**) protein-bound plasma CEL, (**C**) protein-bound BSA MG-H1, (**D**) protein-bound BSA CEL, and MGO after (**E**) 10 μM MGO incubation and (**F**) 100 μM MGO incubation were measured by UPLC-MS/MS. Comparisons of MGO effects on protein-bound MG-H1 or protein-bound CEL formation were tested using two-way ANOVA with Bonferroni's multiple comparison. * represents comparisons with 10 μM MGO, $^{\$}$ represents comparisons with BSA. * indicates $P<0.05$, ** indicates $P<0.01$, and $^{\$\$\$}$ndicates $P<0.001$. Abbreviations: BSA, bovine serum albumin; CEL, N^{ε}-(carboxyethyl)lysine; MG-H1, Nδ-(5-hydro-5-methyl-4-imidazolon-2-yl)-ornithine; MGO, methylglyoxal.

MGO formation in tissues during an intraperitoneal glucose tolerance test is also derived from exogenous glucose in mice

Next, we studied in mice whether exogenous glucose contributes to *in vivo* MGO formation in different organs after an intraperitoneal glucose bolus of universally labelled D(+)^{13}C glucose. Blood glucose levels increased rapidly after the intraperitoneal glucose injection and reached a peak at 30 min (Figure 4A). Plasma $^{13}C_3$ MGO levels (Figure 4B) followed the same trend as glucose, which is in accordance with the findings in humans (Figure 1B). In pancreas,

Clinical Science (2023) **137** 697–706
https://doi.org/10.1042/CS20220753

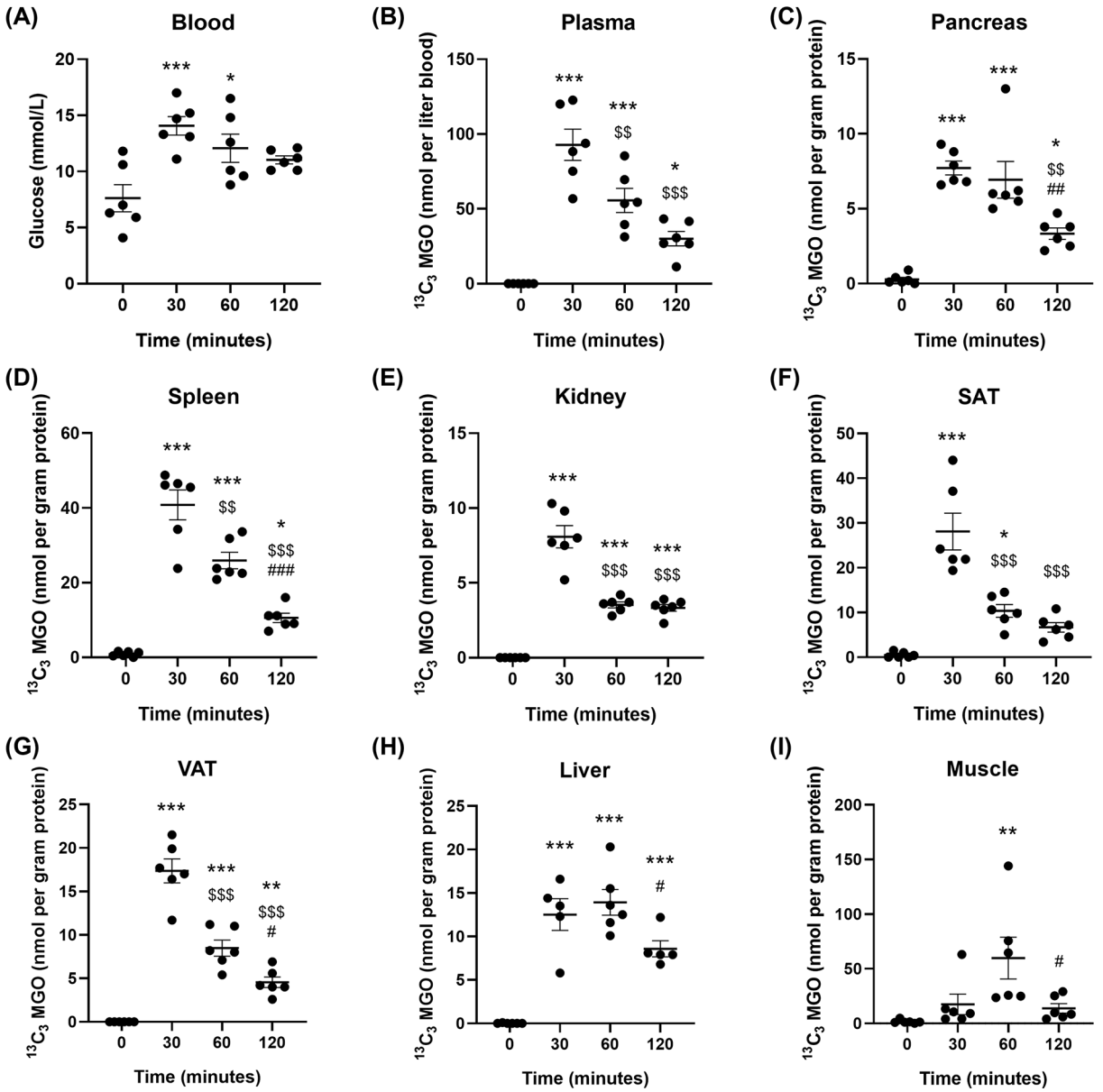

Figure 4. Blood glucose levels and $^{13}C_3$ MGO levels in tissues during a 2-h IPGTT in mice

Glucose levels were measured using a glucometer in (**A**) whole blood. $^{13}C_3$ MGO concentrations were analysed by UPLC-MS/MS, in (**B**) plasma, (**C**) pancreas, (**D**) spleen, (**E**) kidney, (**F**) SAT, (**G**) VAT, (**H**) liver, and (**I**) muscle tissue from C57BL/6J male mice, 10–11 weeks old. Mice were grouped for different time points, n=6 per group. Data are shown as mean ± SEM. Comparisons of glucose levels or $^{13}C_3$ MGO levels at different time points were tested using the ordinary one-way ANOVA with Tukey's multiple comparison. * represents comparisons with time 0, $ represents comparisons with time 30 min, and # represents comparisons with 60 min. */$/# indicates $P<0.05$, **/$$/## indicates $P<0.01$, and ***/$$$/### indicates $P<0.001$. Abbreviations: SAT, subcutaneous adipose tissue; VAT, visceral adipose tissue.

spleen, kidney, SAT, and VAT, $^{13}C_3$ MGO concentrations increased after the glucose bolus, with a peak at 30 min. After this peak, $^{13}C_3$ MGO levels declined, with some residual $^{13}C_3$ MGO in the tissues at 120 min (Figure 4C–G). In the liver and muscle, $^{13}C_3$ MGO formation also increased during the IPGTT with a peak at 60 min (Figure 4H,I). Nonlabelled MGO levels in all the tissues during IPGTT were not affected by the bolus of glucose or slightly decreased at later time points (Supplementary Figure S1). Taken together, these data in mice showed that, similar to plasma,

MGO transiently accumulates in tissues during a glucose tolerance test, and that its formation is directly derived from exogenous glucose.

Discussion

Our study demonstrates that postprandial plasma MGO formation during an OGTT originates from exogenous glucose. This formation of MGO during an OGTT is followed by increased formation of MGO-derived AGEs in plasma. *Ex-vivo* experiments showed that MGO is rapidly decreased when incubated with plasma or BSA, accompanied by a fast formation of MGO-derived AGEs. In mice, we showed that not only the postprandial increase in plasma MGO is derived from exogenous glucose but also MGO formation in pancreas, spleen, kidney, SAT, VAT, liver, and skeletal muscle.

Under physiological conditions, MGO is mainly formed during glycolysis by the nonenzymatic degradation of the glucotrioses glyceraldehyde 3-phosphate and dihydroxyacetone phosphate [13,19], but MGO can also be produced by auto-oxidation of glucose and degradation of glycated proteins [25], catabolism of threonine and acetoacetate [26,27], and lipid peroxidation [28]. In addition to these endogenous sources, MGO can be ingested from food [29]. We previously showed that MGO levels increased rapidly in plasma during an OGTT and a mixed meal test, and that MGO levels followed the trend of glucose curves [16,17], suggesting that increased levels of postprandial glucose are the source of MGO formation in the postprandial phase. Here, we established that the formation of MGO during the OGTT is indeed completely derived from exogenous glucose.

The decrease in $^{13}C_6$ glucose and $^{13}C_3$ MGO levels in plasma after the peak was slower as compared with unlabelled glucose and MGO within 180 min of OGTT, which is most likely due to an overcorrection of the ^{12}C curve in the postprandial phase. The baseline level of ^{12}C glucose is approximately 5 mmol/l and reflects the balance between endogenous production and disposal in fasting state. However, the endogenous production declines rapidly in the postprandial state due to the effects of insulin, to ∼35% of baseline by ∼60 min [17]. By subtracting a fixed baseline level of 5 mmol/l from the total curve of $^{12}C_6$ glucose, this overcorrects the ^{12}C curve, explaining a lower $^{12}C_6$ glucose compared with $^{13}C_6$ glucose curve. This effect becomes most apparent after ∼30–60 min. The same effects play a role for $^{12}C_3$ MGO. The baseline $^{12}C_3$ MGO levels probably reflect the endogenous production of glucose in the liver and muscles by oxidation of glucose/glycogen, which are processes that are also reduced in the postprandial phase. In support of this concept, we observed lower levels of $^{12}C_3$ MGO in mice during the postprandial phase in several tissues including the liver and the muscle. Correction for the baseline MGO levels will again overcorrect the $^{12}C_3$ MGO curve. Although we cannot exclude the possibility that there is also a kinetic isotope effect resulting in lower rates of utilisation of $^{13}C_6$ glucose for glycolysis [30], such an effect is likely too small to explain the observed difference between ^{12}C and ^{13}C patterns of glucose and MGO. In addition, it was also observed that unlabelled glucose and MGO mildly increased again after 180 min of the OGTT, which could be due to a restoration in endogenous glucose formation after being suppressed in the postprandial state.

In agreement with our current findings, we have previously shown a similar increase in the MGO levels in plasma in healthy individuals during OGTT, with a higher increase in plasma MGO in individuals with type 2 diabetes as compared with healthy subjects [17]. Given that glucose spikes have been established as a key driver in the development of diabetic vascular complications [13,18], daily spikes of MGO, as a consequence of postprandial glucose peaks, may explain the effects of glucose spikes.

MGO can react with proteins, resulting in a fast formation of AGEs [24]. Indeed, in the OGTT in humans, we showed a fast increased formation of protein-bound CEL and MG-H1, although the later to a lesser extent. In the *ex-vivo* experiments, we confirmed MGO-induced formation of MG-H1 and CEL in plasma was in a concentration and time-dependent fashion. Interestingly, an incubation of MGO with pure BSA produced MG-H1, but failed to induce protein-bound CEL within 6 h. Since we observed MGO-induced CEL formation in plasma, and since CEL was most profoundly increased during the *in vivo* OGTT in human subjects, the reaction of MGO with lysine in plasma may preferentially be on proteins other than albumin. The low appearance of MG-H1 in plasma *in vivo*, in comparison with the high increase in the formation of MG-H1 *ex vivo*, might be due to a rapid degradation of MG-H1 containing proteins *in vivo* by epithelial cells of renal tubular [31]. In contrast with protein-bound MG-H1 and CEL, free MG-H1 and CEL were decreased over time during the OGTT. We previously found a strong association between dietary AGEs and free AGEs, but not with protein-bound AGEs [32]. Therefore, this decrease in free MG-H1 and CEL during the OGTT most likely reflects the process of the clearance of free AGEs that were derived from food before fasting.

In line with the findings in humans, changes of plasma $^{13}C_3$ MGO levels followed the same pattern as of glucose during IPGTT in mice. Furthermore, an elevation of $^{13}C_3$ MGO levels but not $^{12}C_3$ MGO, after a bolus of glucose was

Clinical Science (2023) **137** 697–706
https://doi.org/10.1042/CS20220753

observed in pancreas, spleen, kidney, SAT, VAT, liver, and muscle, indicating that the increase in MGO in tissues was completely derived from exogenous glucose. The changes of $^{13}C_3$ MGO in the pancreas, spleen, kidney, SAT, and VAT followed the same pattern as for plasma $^{13}C_3$ MGO. Thus, exogenous glucose rapidly results in MGO formation in various tissues. It has been previously demonstrated that glycolysis was largely increased in SAT in the postprandial phase, with only a small increase in pancreas and kidney, and no change in spleen and VAT [33]. Therefore, it might be that the elevated $^{13}C_3$ MGO concentration in spleen and VAT is due to uptake of $^{13}C_3$ MGO from plasma, rather than from glycolysis. The concentrations of $^{13}C_3$ MGO in liver and muscle also increased during the IPGTT, however, with some delay compared with the other tissues. These tissues are very insulin dependent for the uptake of glucose and, therefore, this delay in the formation of $^{13}C_3$ MGO in liver and muscle may reflect the kinetics of insulin release by the pancreas [34]. Another explanation for the relatively later increase in $^{13}C_3$ MGO in the liver and skeletal muscle may be that the intake of glucose is not directly used for glycolysis but first absorbed and used into the glycogen pool, that was likely emptied due to the overnight fasting, before being used for glycolysis [33]. The fact that hepatic $^{12}C_3$ MGO levels declined during IPGTT may be explained by a lower use of the glycogen contribution to glycolysis in the liver.

A limitation of the current study is that only male participants were enrolled in the human study and because of gender differences in response to an OGTT [35], these data may not be completely extrapolated to women.

Overall, we found that postprandial MGO formation during a glucose tolerance test is directly derived from exogenous glucose both in plasma and in tissues, followed by a fast formation of MGO-derived AGEs. MGO stress in the postprandial phase may contribute to the detrimental effects and long-term complications due to postprandial glucose spikes. Reducing MGO stress in the postprandial phase may be a way to reduce the burden of cardiovascular disease in diabetes.

Clinical perspectives

- Background as to why the study was undertaken: plasma MGO levels are linked to cardiometabolic diseases. Increased levels of postprandial MGO in plasma during a glucose tolerance test or a mix meal have been observed, and with a higher increase in individuals with type 2 diabetes. However, the exact source of postprandial MGO is unknown.
- A brief summary of the results: we herein showed that postprandial MGO formation during OGTT is completely derived from exogenous glucose in plasma and in tissues, followed by a fast formation of AGEs in plasma.
- The potential significance to human health and disease: our current findings provide new insights in the formation of MGO in the postprandial phase and this may be of help in lowering MGO stress.

Data Availability

All supporting data are included within the article.

Funding

X.Z. is supported by the China Scholarship Council. Unilever was funder of the human study and provider of the samples from the human study.

CRediT Author Contribution

Xiaodi Zhang: Investigation, Writing—original draft. **Jean L.J.M. Scheijen:** Investigation, Methodology. **Coen D.A. Stehouwer:** Writing—review & editing. **Kristiaan Wouters:** Supervision, Writing—review & editing. **Casper G. Schalkwijk:** Supervision, Project administration, Writing—review & editing.

Acknowledgements

The authors acknowledge Unilever R&D Wageningen for their support of the human study. Unilever was in no way involved with the animal data.

Abbreviations

AGE, advanced glycation endproduct; ANOVA, analysis of variance; BSA, bovine serum albumin; CEL, Nε-(carboxyethyl)lysine; IPGTT, intraperitoneal glucose tolerance test; MG-H1, Nδ-(5-hydro-5-methyl-4-imidazolon-2-yl)-ornithine; MGO, methylglyoxal; OGTT, oral glucose tolerance test; SAT, subcutaneous adipose tissue; SEM, standard error of the mean; UPLC-MS/MS , ultra-performance liquid chromatography-tandem mass spectrometry; VAT, visceral adipose tissue.

References

1 Brownlee, M. (1995) Advanced protein glycosylation in diabetes and aging. *Annu. Rev. Med.* **46**, 223–234, https://doi.org/10.1146/annurev.med.46.1.223
2 Thornalley, P.J., Battah, S., Ahmed, N., Karachalias, N., Agalou, S., Babaei-Jadidi, R. et al. (2003) Quantitative screening of advanced glycation endproducts in cellular and extracellular proteins by tandem mass spectrometry. *Biochem. J.* **375**, 581–592, https://doi.org/10.1042/bj20030763
3 Ahmed, M.U., FRYE, E.B., Degenhardt, T.P., Thorpe, S.R. and Baynes, J.W. (1997) N ε-(carboxyethyl) lysine, a product of the chemical modification of proteins by methylglyoxal, increases with age in human lens proteins. *Biochem. J.* **324**, 565–570, https://doi.org/10.1042/bj3240565
4 Takahashi, K. (1977) The reactions of phenylglyoxal and related reagents with amino acids. *J. Biochem.* **81**, 395–402, https://doi.org/10.1093/oxfordjournals.jbchem.a131471
5 Morcos, M., Du, X., Pfisterer, F., Hutter, H., Sayed, A.A., Thornalley, P. et al. (2008) Glyoxalase-1 prevents mitochondrial protein modification and enhances lifespan in Caenorhabditis elegans. *Aging Cell* **7**, 260–269, https://doi.org/10.1111/j.1474-9726.2008.00371.x
6 Dobler, D., Ahmed, N., Song, L., Eboigbodin, K.E. and Thornalley, P.J. (2006) Increased dicarbonyl metabolism in endothelial cells in hyperglycemia induces anoikis and impairs angiogenesis by RGD and GFOGER motif modification. *Diabetes* **55**, 1961–1969, https://doi.org/10.2337/db05-1634
7 Chan, W.H., Wu, H.J. and Shiao, N.H. (2007) Apoptotic signaling in methylglyoxal-treated human osteoblasts involves oxidative stress, c-Jun N-terminal kinase, caspase-3, and p21-activated kinase 2. *J. Cell. Biochem.* **100**, 1056–1069, https://doi.org/10.1002/jcb.21114
8 Hanssen, N.M., Wouters, K., Huijberts, M.S., Gijbels, M.J., Sluimer, J.C., Scheijen, J.L. et al. (2014) Higher levels of advanced glycation endproducts in human carotid atherosclerotic plaques are associated with a rupture-prone phenotype. *Eur. Heart J.* **35**, 1137–1146, https://doi.org/10.1093/eurheartj/eht402
9 Stratmann, B., Engelbrecht, B., Espelage, B.C., Klusmeier, N., Tiemann, J., Gawlowski, T. et al. (2016) Glyoxalase 1-knockdown in human aortic endothelial cells–effect on the proteome and endothelial function estimates. *Sci. Rep.* **6**, 1–16, https://doi.org/10.1038/srep37737
10 Brouwers, O., Niessen, P.M., Miyata, T., Østergaard, J.A., Flyvbjerg, A., Peutz-Kootstra, C.J. et al. (2014) Glyoxalase-1 overexpression reduces endothelial dysfunction and attenuates early renal impairment in a rat model of diabetes. *Diabetologia* **57**, 224–235, https://doi.org/10.1007/s00125-013-3088-5
11 Maessen, D.E.M., Stehouwer, C.D.A. and Schalkwijk, C.G. (2015) The role of methylglyoxal and the glyoxalase system in diabetes and other age-related diseases. *Clin. Sci.* **128**, 839–861, https://doi.org/10.1042/CS20140683
12 Brouwers, O., Niessen, P.M., Ferreira, I., Miyata, T., Scheffer, P.G., Teerlink, T. et al. (2011) Overexpression of glyoxalase-I reduces hyperglycemia-induced levels of advanced glycation end products and oxidative stress in diabetic rats. *J. Biol. Chem.* **286**, 1374–1380, https://doi.org/10.1074/jbc.M110.144097
13 Schalkwijk, C.G. and Stehouwer, C.D.A. (2020) Methylglyoxal, a highly reactive dicarbonyl compound, in diabetes, its vascular complications, and other age-related diseases. *Physiol. Rev.* **100**, 407–461, https://doi.org/10.1152/physrev.00001.2019
14 Hanssen, N.M., Westerink, J., Scheijen, J.L., Van Der Graaf, Y., Stehouwer, C.D., Schalkwijk, C.G. et al. (2018) Higher plasma methylglyoxal levels are associated with incident cardiovascular disease and mortality in individuals with type 2 diabetes. *Diabetes Care.* **41**, 1689–1695, https://doi.org/10.2337/dc18-0159
15 Hanssen, N., Scheijen, J., Houben, A., van de Waarenburg, M., Berendschot, T., Webers, C. et al. (2021) Fasting and post-oral-glucose-load levels of methylglyoxal are associated with microvascular, but not macrovascular, disease in individuals with and without (pre) diabetes: the Maastricht Study. *Diab. Metab.* **47**, 101148, https://doi.org/10.1016/j.diabet.2020.02.002
16 Maessen, D.E., Hanssen, N.M., Lips, M.A., Scheijen, J.L., van Dijk, K.W., Pijl, H. et al. (2016) Energy restriction and Roux-en-Y gastric bypass reduce postprandial α-dicarbonyl stress in obese women with type 2 diabetes. *Diabetologia* **59**, 2013–2017, https://doi.org/10.1007/s00125-016-4009-1
17 Maessen, D.E., Hanssen, N.M., Scheijen, J.L., van der Kallen, C.J., van Greevenbroek, M.M., Stehouwer, C.D. et al. (2015) Post–glucose load plasma α-dicarbonyl concentrations are increased in individuals with impaired glucose metabolism and type 2 diabetes: the CODAM study. *Diabetes Care.* **38**, 913–920, https://doi.org/10.2337/dc14-2605
18 Hanssen, N.M., Kraakman, M.J., Flynn, M.C., Nagareddy, P.R., Schalkwijk, C.G. and Murphy, A.J. (2020) Postprandial glucose spikes, an important contributor to cardiovascular disease in diabetes? *Front. Cardiovasc. Med.* **7**, 168, https://doi.org/10.3389/fcvm.2020.570553
19 Phillips, S.A. and Thornalley, P.J. (1993) The formation of methylglyoxal from triose phosphates: investigation using a specific assay for methylglyoxal. *Eur. J. Biochem.* **212**, 101–105, https://doi.org/10.1111/j.1432-1033.1993.tb17638.x
20 Richard, J. (1993) Mechanism for the formation of methylglyoxal from triosephosphates. *Biochem. Soc. Trans.* **21**, 549–553, https://doi.org/10.1042/bst0210549
21 Scheijen, J.L. and Schalkwijk, C.G. (2014) Quantification of glyoxal, methylglyoxal and 3-deoxyglucosone in blood and plasma by ultra performance liquid chromatography tandem mass spectrometry: evaluation of blood specimen. *Clin. Chem. Lab. Med.* **52**, 85–91, https://doi.org/10.1515/cclm-2012-0878
22 Martens, R.J., Broers, N.J., Canaud, B., Christiaans, M.H., Cornelis, T., Gauly, A. et al. (2019) Relations of advanced glycation endproducts and dicarbonyls with endothelial dysfunction and low-grade inflammation in individuals with end-stage renal disease in the transition to renal replacement therapy: a cross-sectional observational study. *PloS ONE* **14**, e0221058, https://doi.org/10.1371/journal.pone.0221058

Clinical Science (2023) **137** 697–706
https://doi.org/10.1042/CS20220753

23 Rabbani, N. and Thornalley, P.J. (2014) Measurement of methylglyoxal by stable isotopic dilution analysis LC-MS/MS with corroborative prediction in physiological samples. *Nat. Protoc.* **9**, 1969–1979, https://doi.org/10.1038/nprot.2014.129
24 Rabbani, N. and Thornalley, P.J. (2012) Methylglyoxal, glyoxalase 1 and the dicarbonyl proteome. *Amino Acids* **42**, 1133–1142, https://doi.org/10.1007/s00726-010-0783-0
25 Thornalley, P.J., Langborg, A. and Minhas, H.S. (1999) Formation of glyoxal, methylglyoxal and 3-deoxyglucosone in the glycation of proteins by glucose. *Biochem. J.* **344**, 109–116, https://doi.org/10.1042/bj3440109
26 Reichard, G., Skutches, C., Hoeldtke, R. and Owen, O. (1986) Acetone metabolism in humans during diabetic ketoacidosis. *Diabetes* **35**, 668–674, https://doi.org/10.2337/diab.35.6.668
27 Ray, M. and Ray, S. (1987) Aminoacetone oxidase from goat liver. Formation of methylglyoxal from aminoacetone. *J. Biol. Chem.* **262**, 5974–5977, https://doi.org/10.1016/S0021-9258(18)45524-X
28 Baynes, J.W. and Thorpe, S.R. (2000) Glycoxidation and lipoxidation in atherogenesis. *Free Radic. Biol. Med.* **28**, 1708–1716, https://doi.org/10.1016/S0891-5849(00)00228-8
29 Maasen, K., Eussen, S.J., Scheijen, J.L., van der Kallen, C.J., Dagnelie, P.C., Opperhuizen, A. et al. (2021) Higher habitual intake of dietary dicarbonyls is associated with higher corresponding plasma dicarbonyl concentrations and skin autofluorescence: the Maastricht Study. *Am. J. Clin. Nutr.* **115**, 34–44, https://doi.org/10.1093/ajcn/nqab329
30 Wasylenko, T.M. and Stephanopoulos, G. (2013) Kinetic isotope effects significantly influence intracellular metabolite 13C labeling patterns and flux determination. *Biotechnol. J.* **8**, 1080–1089, https://doi.org/10.1002/biot.201200276
31 Gugliucci, A. and Bendayan, M. (1996) Renal fate of circulating advanced glycated end products (AGE): evidence for reabsorption and catabolism of AGE-peptides by renal proximal tubular cells. *Diabetologia* **39**, 149–160, https://doi.org/10.1007/BF00403957
32 Scheijen, J.L., Hanssen, N.M., van Greevenbroek, M.M., Van der Kallen, C.J., Feskens, E.J., Stehouwer, C.D. et al. (2018) Dietary intake of advanced glycation endproducts is associated with higher levels of advanced glycation endproducts in plasma and urine: the CODAM study. *Clin. Nutr.* **37**, 919–925, https://doi.org/10.1016/j.clnu.2017.03.019
33 TeSlaa, T., Bartman, C.R., Jankowski, C.S., Zhang, Z., Xu, X., Xing, X. et al. (2021) The source of glycolytic intermediates in mammalian tissues. *Cell Metab.* **33**, 367.e5–378.e5, https://doi.org/10.1016/j.cmet.2020.12.020
34 Röder, P.V., Wu, B., Liu, Y. and Han, W. (2016) Pancreatic regulation of glucose homeostasis. *Exp. Mol. Med.* **48**, e219–e, https://doi.org/10.1038/emm.2016.6
35 Sicree, R., Zimmet, P., Dunstan, D., Cameron, A., Welborn, T. and Shaw, J. (2008) Differences in height explain gender differences in the response to the oral glucose tolerance test—the AusDiab study. *Diabet. Med.* **25**, 296–302, https://doi.org/10.1111/j.1464-5491.2007.02362.x

Supplementary data

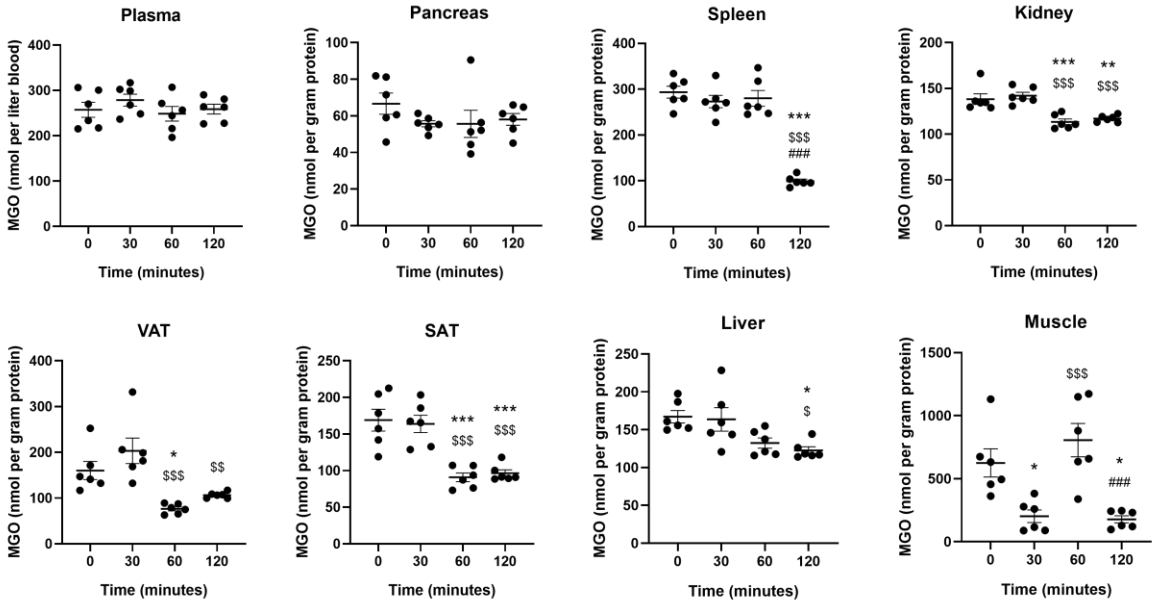

Figure S1. MGO levels in tissues during a 2-hour IPGTT in mice. MGO concentrations were analysed by UPLC-MS/MS, in plasma, pancreas, spleen, kidney, SAT, VAT, liver, and muscle tissues from C57BL/6J male mice, 10-11 weeks old. Mice were grouped for different time points, n=6 per group. Data are shown as mean ± SEM. Comparisons of MGO levels at different time points were tested using the ordinary one-way ANOVA with Tukey's multiple comparison. * represents comparisons with time 0, $ represents comparisons with time 30 min, and # represents comparisons with 60 min. */$/# indicates $p<0.05$, **/$$/## indicates $p<0.01$, and ***/$$$/### indicates $p<0.001$.